Available online at www.sciencedirect.com
SCIENCE DIRECT
Journal of Catalysis 237 (2006) 267–277
JOURNAL OF CATALYSIS
www.elsevier.com/locate/jcat

Hydrothermal stabilization of ZSM-5 catalytic-cracking additives by phosphorus addition

T. Blasco, A. Corma *, J. Martínez-Triguero

Instituto de Tecnología Química (UPV-CSIC), Universidad Politécnica de Valencia, Avenida de los Naranjos s/n, 46022 Valencia, Spain

Received 28 July 2005; revised 9 November 2005; accepted 10 November 2005

Abstract

ZSM-5 zeolites with different Si/Al ratios (15, 25, 40) were impregnated with phosphorus (0.5–3 wt%) in form of H_3PO_4 or $NH_4H_2PO_4$. The samples were characterized before and after severe hydrothermal treatment by XRD, IR, ^{27}Al, ^{29}Si, ^{31}P MAS NMR, and their activity for the cracking of *n*-decane was measured. It was found that phosphorus impregnation increases the hydrothermal stability of framework aluminum whatever the source of phosphorus used. The acidity and cracking activity of steamed samples reached an optimum for a P/Al molar ratio of ca. 0.5–0.7. A chemical model for the phosphorus–zeolite interaction is proposed in which the framework aluminum pairs are stabilized by extra-framework cationic species formed by protonation of orthophosphoric acid. The influence of isolated versus pairs of aluminum on activity and selectivity after steaming is discussed. When P-impregnated ZSM-5 sample is used as an additive for cracking industrial feeds, selectivity to propylene and butenes increases.

Keywords: ZSM-5 Hydrothermal stability; Phosphorus stabilized ZSM-5; Zeolite cracking additive; Single isolated and Al pairs in zeolites

1. Introduction

Zeolites are widely used as catalysts, and there is an incentive to find new structures with differing pore dimensions and topologies [1–8]. The hydrothermal stability of zeolite catalysts is especially important in fluid catalytic cracking (FCC). In this process, the catalyst is subjected to regeneration temperatures above 800 °C in the presence of steam, and its activity strongly decays after several cycles of reaction–regeneration until reaching an "equilibrium" state. This loss of activity is related to the dealumination of the zeolitic framework and the corresponding decrease of Brönsted acidity. Preventing or decreasing this dealumination is a topic of continuous interest in the field of zeolite catalysts, specifically in FCC applications.

Synthesized in the sodium form, zeolites are hydrothermally stable but have no acid properties; therefore, they are not active for hydrocarbon cracking. But acid zeolites tend to reach a state of minimum energy by expelling aluminum out of the framework, producing pure silica zeolites and alumina. In zeolite Y, framework stabilization was first achieved by exchanging sodium ions with rare earth cations. It was found that Lanthanum cations stabilize the unit cell at higher values, maintaining more aluminum in framework positions [9–12]. Introducing phosphorus to increase the attrition resistance of the catalyst particles also increased the hydrothermal stability of the ZSM-5 zeolite additive, with an Al content lower than Y, toward dealumination [13–15]. Since then, the composition of most FCC and ZSM-5 catalyst additives includes phosphorus.

The interaction between phosphorus and zeolite Y [16], and especially ZSM-5 [17–27], has been investigated by several groups. For zeolite Y, it was found that phosphorus added in the form of H_3PO_4 reacted with framework and extra-framework aluminum, forming different surface aluminophosphates that change the acid properties of the resultant zeolite [16]. In the case of zeolite ZSM-5 [17–27], P compounds interact with bridged OH groups, decreasing zeolite acidity and, consequently, catalytic activity and modifying shape selectivity. Caro et al. [28] explained this acidity reduction by framework dealumination and formation of aluminum phosphate; however, Seo et al. [29] observed no any dealumination after phosphorus

* Corresponding author. Fax: +34 96 387 7809.
E-mail address: acorma@itq.upv.es (A. Corma).

0021-9517/$ – see front matter
doi:10.1016/j.jcat.2005.11.011

treatment, and they attributed the reduction of Brönsted acidity to the formation of octahedral aluminum through its interaction with phosphorus. Lischke et al. [30,31] showed that more Brönsted acid sites are preserved after hydrothermal treatment of phosphorus-impregnated ZSM-5. Moreover, additional Brönsted acid sites are recovered after hot water washing and elution of the phosphorus-treated zeolite [31]. More recently, Zhuang et al. [32] proposed that P can occupy framework silicon positions to form $(SiO)_xAl(PO)_{4-x}$ species after hydrothermal treatment of ZSM-5 stabilized with phosphorus and lanthanum. Therefore, although there is a general agreement on the stabilization of framework aluminum by phosphorus addition, controversy exists as to how P interacts with zeolite and as to whether or not P occupies framework positions. Moreover, some other fundamental questions remain to be answered, including the nature of the phosphorus compounds responsible for the stabilization of framework aluminum, and the influence of catalyst variables, such as phosphorus content, initial Si/Al zeolite ratio, and the presence of extra-framework aluminum, on the Brönsted acidity remaining after hydrothermal treatment.

In this work we investigated the influence of the amount of P and the impregnated agent on the stabilization of the framework aluminum in ZSM-5. The steam-equilibrated P-ZSM-5 samples were tested as catalysts in the cracking of *n*-decane and as an FCC component in the cracking of a commercial gasoil. The postsynthesis conditions that give the optimum P-modified FCC additive were optimized. The results from the spectroscopic characterization of phosphorus-treated and steam-equilibrated ZSM-5 samples were correlated with the catalytic cracking results in an attempt to answer the aforementioned questions.

2. Experimental

2.1. Materials

ZSM-5 samples with varying Si/Al ratios (Table 1) were obtained from Zeolyst. Phosphorus was impregnated from an aqueous solution of either $NH_4H_2PO_4$ (Aldrich, 99.8%) or H_3PO_4 (Aldrich, 85% in water). The amount of phosphorus varied between 0.25 and 3 wt% in P. The impregnation methodology was as follows: 1 g of the parent ZSM5 was suspended in a solution of milli-Q water containing the phosphorus compound with a liquid-to-solid ratio 10 (wt/wt). The amount of phosphorus was calculated on the basis of the final weight of P desired on the zeolite. The suspension was slowly evaporated (for 1 h) in a rotary vacuum evaporator at 80 °C until dry. Then the samples were dried for another 2 h at 100 °C and calcined for 1 h at 500 °C. Steaming was done at 750 °C for 5 h in 100% steam.

Table 1
Nomenclature and physicochemical characteristics of parent ZSM-5 samples used in this work

	Commercial code	Si/Al	Crystal size (μm)	BET surface area ($m^2\,g^{-1}$)
15-ZSM5	CBV3020	15	0.1	393
25-ZSM5	CBV5020	25	0.1	414
40-ZSM5	CBV8020	40	0.5–1	409

The samples were identified as "ZSM5" preceded by the Si/Al ratio and followed by the P content, expressed in wt%. When the source of P was orthophosphoric acid, an "A" was added. The steamed samples were identified by a final "St."

2.2. Sample characterization

Bulk Si/Al ratio was determined by atomic absorption spectrophotometry using a SpectraA-Plus apparatus (Varian). Textural properties were measured by N_2 adsorption at −196 °C on a Micromeritics ASAP-2000 apparatus after the samples were pretreated at 400 °C under vacuum overnight. Infrared (IR) experiments were performed using vacuum cells. Wafers of 10 mg cm^{-2} thickness were degassed overnight under vacuum (10^{-3} Pa) at 400 °C. Then pyridine (6×10^{-2} Pa) was admitted, and, after equilibration, the samples were outgassed for 1 h at increasing temperatures (150, 250, and 350 °C). The spectra were recorded at room temperature before pyridine adsorption and after each desorption step, and the background was subtracted. Relative determination of Brönsted and Lewis acidity was derived from the area of the IR bands at ca. 1450 and 1550 cm^{-1}, respectively, using the extinction coefficients given by Emeis [33] and considering the number of Brönsted acid sites adsorbed at 150 °C on the 15-ZSM5 sample to be 100.

Solid-state ^{29}Si NMR spectra were recorded under magic angle spinning (MAS) at room temperature in a Varian Unity VXR-400WB spectrometer, with a spinning rate of 5 kHz at 79.459 MHz with a 55° pulse length of 3.5 μs and repetition time of 40 s. Cross-polarization measurements were done at 5 kHz, using a 90° pulse for protons of 9 μs, 3.0 ms of contact time, and 3 s of recycle delay. Chemical shifts were reported relative to tetramethylsilane. Solid State ^{27}Al NMR spectra were recorded at 104.2 MHz with a spinning rate of 7 kHz and a 9° pulse length of 0.5 μs with a 0.5 s repetition time. ^{27}Al chemical shifts were reported relative to $[Al^{3+}(H_2O)_6]$. Solid-state ^{31}P NMR spectra were recorded at 161.9 MHz with a spinning rate of 7 kHz and a 67.5° pulse length of 4.9 μs with 15 s repetition time. The chemical shifts were reported relative to 85% H_3PO_4.

2.3. Reaction procedure

n-Decane cracking experiments were performed at 500 °C and for 60 s time on stream in a microactivity test unit as described previously [34]. Zeolites were pelletized, crushed, and sieved, and the 0.59- to 0.84-mm fraction was taken and diluted in 2.5 g of inert silica. For each catalyst, five experiments were performed, maintaining the amount of catalyst (cat) constant and equal to 0.5 g and varying the *n*-decane amount (oil) between 0.77 and 1.54 g. Kinetic rate constants were calculated by fitting the conversions (X) to a first-order kinetic equation for a plug flow reactor (1), assuming that the deactivation is enclosed in the kinetic constant and taking into account the volumetric expansion factor (2),

$$K = -\left(\text{cat oil}^{-1}\text{TOS}\right)^{-1}\left[\varepsilon X + (1+\varepsilon)\ln(1-X)\right], \qquad (1)$$

Table 2
Vacuum gasoil properties

Density (60 °C) (g ml^{-1})	0.916
Aniline point (°C)	76
Sulfur (wt%)	2.7
Nitrogen (wt%)	0.15
Carbon conradson (%)	0.09
Na (ppm)	<0.05
Cu (ppm)	30
Fe (ppm)	0.5
Ni (ppb)	30
V (ppb)	<25
ASTM D-1160 (°C)	
10%	400
30%	411
50%	425
70%	449
90%	489

$$\varepsilon = \left(\sum \text{molar selectivities of products}\right) - 1. \quad (2)$$

The cracking of vacuum gasoil (Table 2) was performed at 520 °C and 30 s time on stream following the methodology described previously [34], where ZSM-5 is tested as an additive of USY zeolite (CBV760 from Zeolyst, unit cell 2.426 nm).

3. Results and discussion

3.1. Acidity measurements

The acidity of the ZSM-5 zeolites with varying Si/Al ratios impregnated with $NH_4H_2PO_4$ or H_3PO_4, before and after steaming, were measured using FTIR spectroscopy and pyridine as a probe molecule. The results obtained for all of the samples, summarized in Tables 3–5, demonstrate that before steaming, the incorporation of phosphorus reduces the acidity regardless of the starting phosphorus compound (see, e.g., sample 25-ZSM5 in Table 4). Even small amounts (e.g., 0.25 wt% of P in 25-ZSM5) decrease pyridine adsorption by 30%. Zeolite acidity decreases with P content, more so when H_3PO_4 instead of $NH_4H_2PO_4$ is used as phosphorus source (zeolite 25-ZSM5 in Table 4). The pyridine desorption at increasing temperatures reveals that P impregnation preferentially reduces the number of the stronger acid sites, that is, those that still adsorb pyridine at 350 °C.

The changes in zeolite acidity resulting from phosphorus impregnation should be reflected in the bridging hydroxyl groups of the zeolite. This is illustrated in Fig. 1 for zeolite 25-ZSM5 impregnated with different amounts of $NH_4H_2PO_4$. The FTIR spectrum of phosphorus-free zeolite 25-ZSM5 shows bands at 3740, 3600–3610, and 3665 cm^{-1}, corresponding to external silanols, bridged hydroxyls, and hydroxyl groups bonded to extra-framework alumina, respectively. After P impregnation and subsequent calcination (Fig. 1A), the bands at 3610 cm^{-1}, accounting for the sample acidity, and at 3665 cm^{-1} decrease with increasing P content. Meanwhile, another band at 3676 cm^{-1}, assigned to phosphorus hydroxyl groups in amorphous aluminum phosphates [19,35,36] and also appearing in P-impregnated USY zeolites [16], arises. Some of these P–OH groups interact with pyridine showing a Brönsted acidic character. Similar spectral features are seen for 15-ZSM5 and 40-ZSM5 samples with varying amounts of P (not shown).

After steaming, a strong reduction of the overall acidity occurs (Tables 3–5), which is smaller at higher P content, in contrast to what it was observed after calcination. Again, no differences are observed when $NH_4H_2PO_4$ or H_3PO_4 are used to impregnate zeolite 25-ZSM5. Fig. 1B shows the hydroxyl IR region of steamed P-containing 25-ZSM5-P samples. All spectra show an intense signal at 3740 cm^{-1} of isolated silanol groups; however, the band at 3600 cm^{-1} of Brönsted acid sites is absent in the P-free zeolite but still observed in the P-containing samples. The band at 3675 cm^{-1}, assigned to P–OH groups, increases progressively with P content, at least up to 1 wt% P.

To gain further insight into the nature of the phosphorus species formed on the zeolite impregnation, sample 25-ZSM5-1PSt was washed with NH_4Cl or NH_4F. This treatment restored part of the zeolite acidity (Table 6), indicating the removal of

Table 3
Textural and acidity properties of 15-ZSM5 Si/Al = 15 impregnated with P in form of $NH_4H_2PO_4$ fresh and steamed

Sample	BET surface area (m^2 g^{-1})	Micropore volume (ml g^{-1})	Brönsted acidity			Lewis acidity		
			150 °C	250 °C	350 °C	150 °C	250 °C	350 °C
15-ZSM5	393	0.160	100	76	39	28	20	14
15-ZSM5-0.5P	372	0.152	80	65	21	17	14	8
15-ZSM5-1P	344	0.137	65	55	31	14	13	8
15-ZSM5-1.5P	328	0.130	51	39	24	8	8	7
15-ZSM5-2P	314	0.125	48	38	14	8	6	4
15-ZSM5-2.5P	288	0.115	54	32	7	10	6	4
15-ZSM5-3P	263	0.104	28	20	3	3	1	1
15-ZSM5-St	326	0.135	7	3	1	7	4	3
15-ZSM5-0.5PSt	332	0.142	8	4	0	6	4	1
15-ZSM5-1PSt	338	0.142	7	3	0	6	4	3
15-ZSM5-1.5PSt	334	0.140	8	3	1	4	4	3
15-ZSM5-2PSt	339	0.143	11	8	3	7	7	4
15-ZSM5-2.5PSt	334	0.139	12	7	1	6	3	3
15-ZSM5-3PSt	323	0.135	14	6	1	3	1	1

Table 4
Textural and acidity properties of ZSM-5 Si/Al = 25 impregnated with P in form of $NH_4H_2PO_4$ (P) or H_3PO_4 (A) fresh and steamed

Sample	BET surface area ($m^2\ g^{-1}$)	Micropore volume ($ml\ g^{-1}$)	Brönsted acidity			Lewis acidity		
			150 °C	250 °C	350 °C	150 °C	250 °C	350 °C
25-ZSM5	414	0.165	97	93	80	11	11	11
25-ZSM5-0.25P	410	0.163	83	80	68	10	8	7
25-ZSM5-0.5P	404	0.160	65	54	39	7	4	4
25-ZSM5-1P	373	0.147	48	41	31	6	4	4
25-ZSM5-2P	330	0.127	39	25	13	3	1	1
25-ZSM5-0.25A	412	0.164	89	80	66	4	3	3
25-ZSM5-0.5A	406	0.162	72	68	54	6	4	1
25-ZSM5-1A	376	0.155	28	20	17	3	1	1
25-ZSM5-2A	330	0.134	21	13	8	1	1	1
25-ZSM5-St	322	0.101	6	1	0	10	6	3
25-ZSM5-0.25PSt	328	0.110	8	3	1	10	7	4
25-ZSM5-0.5PSt	333	0.122	7	6	1	7	7	4
25-ZSM5-1PSt	330	0.138	8	8	3	7	7	6
25-ZSM5-2PSt	342	0.142	10	8	3	3	3	1
25-ZSM5-0.25ASt	322	0.108	7	3	1	6	4	3
25-ZSM5-0.5ASt	348	0.144	7	3	1	6	4	3
25-ZSM5-1ASt	338	0.138	10	8	3	6	6	6
25-ZSM5-2ASt	332	0.136	10	8	3	1	1	1

Table 5
Textural and acidity properties of ZSM-5 Si/Al = 40 impregnated with different amounts of P in form of $NH_4H_2PO_4$ fresh and steamed

Sample	BET surface area ($m^2\ g^{-1}$)	Micropore volume ($ml\ g^{-1}$)	Brönsted acidity			Lewis acidity		
			150 °C	250 °C	350 °C	150 °C	250 °C	350 °C
40-ZSM5	409	0.174	68	55	30	11	11	11
40-ZSM5-0.25P	387	0.163	51	42	23	10	10	10
40-ZSM5-0.5P	378	0.159	45	34	17	6	6	6
40-ZSM5-0.75P	369	0.155	32	25	13	4	3	3
40-ZSM5-1P	367	0.154	41	31	20	4	3	1
40-ZSM5-1.5P	351	0.147	30	21	8	3	1	1
40-ZSM5-St	349	0.157	3	0	0	4	1	0
40-ZSM5-0.25PSt	354	0.162	3	1	0	1	0	0
40-ZSM5-0.5PSt	364	0.164	4	1	0	3	1	1
40-ZSM5-0.75PSt	371	0.164	7	3	1	3	1	1
40-ZSM5-1PSt	381	0.166	9	6	3	2	1	1
40-ZSM5-1.5PSt	389	0.166	10	6	1	1	1	1

some species interacting with the bridging hydroxyl groups. Therefore, the diminution of the zeolite acidity observed after P impregnation must not be due solely to framework dealumination.

We need to point out that we observed no pore blocking, at least not to the extent where it significantly reduced N_2 adsorption or kept pyridine from interacting with acid sites. Indeed, a maximum reduction of ∼20% in BET surface area and micropore volume was observed. Moreover, the disappearance of the IR band at ca. 3600 cm^{-1} after pyridine adsorption indicates that this molecule has access to the bridged hydroxyls located in the zeolite channels.

Thus, from the textural and acidity characterization results, we can conclude the following: (i) The introduction of P does not produce any important pore blockage, at least for P content ⩽3 wt%; (ii) impregnation of ZSM-5 with P and subsequent calcination produces a reduction in the number of acid sites, especially those with stronger acidity; and (iii) after steaming, phosphorus-containing samples retain more acid sites than unmodified ZSM-5.

3.2. Solid-state NMR results

Fig. 2 shows the ^{29}Si MAS NMR spectra of zeolites 25-ZSM5, 25-ZSM5-1P, and 25-ZSM5-2P, calcined and after steaming. The spectra of the calcined samples show a broad peak at ∼ −113 ppm and a shoulder at −115 ppm, both assigned to Si(4Si) units, and another broad signal at a lower field. The spectra decomposition into individual Gaussian lines indicates that the low field component is formed by two peaks, at −105 and −102 ppm, attributed to Si(3Si1Al) and structural defects of Si(3SiOH) type [34], respectively. The Si/Al ratio estimated from the spectra simulation is in the range of 35–40 for the P-free and P-containing calcined samples. Therefore, no important differences in framework dealumination during calcination are appreciable by ^{29}Si NMR when zeolite ZSM-5 is modified with P.

Different results are obtained with the steamed samples, as shown in Fig. 2. Whereas a drastic change is observed in the spectrum of the P-free 25-ZSM5, only a slight decrease in the intensity of the low field component is observed for samples 25-

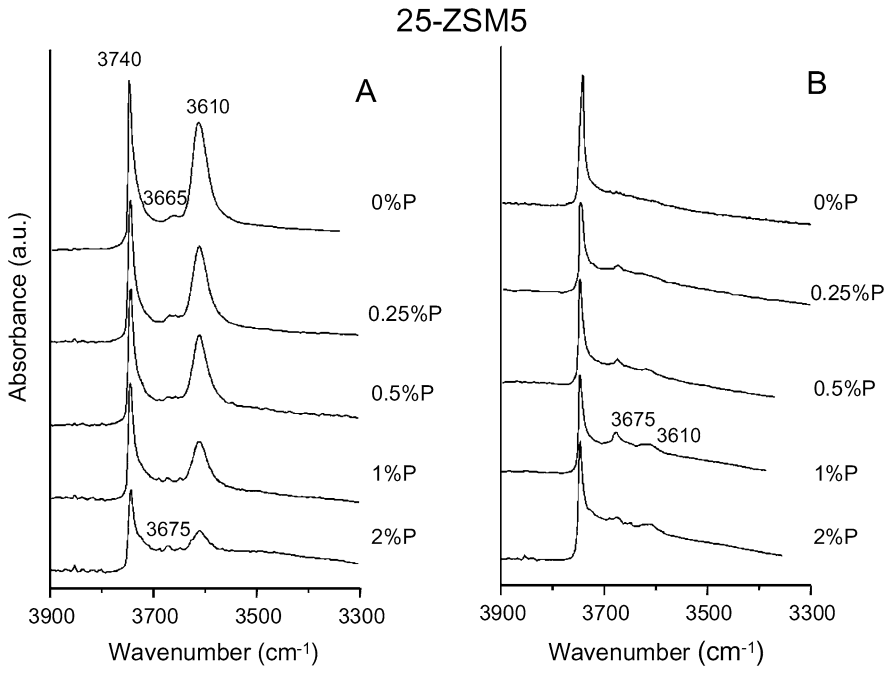

Fig. 1. FTIR spectra of P-free and P-containing zeolite 25-ZSM5 degassed at 400 °C, prepared by impregnation with $NH_4H_2PO_4$ (A) calcined and (B) subsequent steaming at 750 °C 5 h.

Table 6
Acidity, chemical analysis and textural properties of 25-ZSM5-1PSt and 25-ZSM5-St, washed for 3 h at 100 °C in a solution of NH_4Cl or NH_4F

Sample	BET surface area ($m^2\ g^{-1}$)	Micropore volume ($ml\ g^{-1}$)	Al (wt%)	P (wt%)	Si/Al	Brönsted acidity			Lewis acidity		
						150 °C	250 °C	350 °C	150 °C	250 °C	350 °C
25-ZSM5-1PSt	330	0.138	1.74	1	25	8	8	3	7	7	6
25-ZSM5-1PSt (NH_4F washed)	352	0.140	0.81	0.06	54	27	24	7	11	10	6
25-ZSM5-1PSt (NH_4Cl washed)	337	0.134	1.14	0.59	38	23	17	7	10	10	7
25-ZSM5-St (NH_4F washed)	333	0.129	0.74	0	60	7	3	0	8	6	3
25-ZSM5-St (NH_4Cl washed)	324	0.124	1.24	0	36	7	1	0	8	6	3

ZSM5-1PSt and 25-ZSM5-2PSt. The spectrum of zeolite 25-ZSM5-St contains no signal of Si atoms with Al in its second coordination shell, and the Si(4Si) region is highly resolved, making it possible to distinguish at least eight peaks, which is typical of ZSM-5 with a Si/Al ratio > 1000. These changes clearly indicate that large framework dealumination occurs in the unmodified ZSM-5 after steaming, whereas only partial framework dealumination occurs in the P-containing samples.

Fig. 3 shows the ^{27}Al MAS NMR spectra of the P-free and P-containing zeolite 25-ZSM5 before and after steaming. The spectrum of the calcined parent zeolite consists of an intense signal at 54 ppm of tetrahedral Al at the zeolite framework, and another, weaker signal at 0 ppm typical of extra-framework octahedral aluminum. Similar spectra are obtained for the calcined P-containing 25-ZSM5 samples (from $NH_4H_2PO_4$), but the relatively weak signal of octahedral Al appears now at −14 ppm instead of 0 ppm, and a broad band becomes evident at ca. 36 ppm. The latter signal is usually attributed to tetrahedral aluminum in a distorted environment at either framework [37] or non-framework [38–40] positions. Moreover, we cannot discard the presence of penta-coordinated species appearing in the same region in the one-dimensional ^{27}Al NMR spectrum [32,37,38,40].

After the parent zeolite is steamed, the signal of framework Al decreases and a new broad band at ca. 30 ppm of distorted tetrahedral Al appears. A similar effect occurs after the P-containing zeolites are steamed: a decrease in framework Al and an increase in the signals of octahedral aluminum and the band in the intermediate region of 30–40 ppm. The maximum of the later signal shifts to low fields as the P content increases, appearing at 30 ppm for sample 25-ZSM5-0.5PSt and at 40 ppm for 25-ZSM5-2PSt. The two high field signals were previously identified in ZSM-5 and Y zeolite modified with orthophosphoric acid [16,30,31]; however, its assignment remains controversial. The signals at 40 and −16 ppm have been attributed to tetrahedral and octahedral Al coordinated with water, respectively, in an extra-framework aluminum phosphate [28,31,32,41,42]. The signal at 40 ppm has also been ascribed

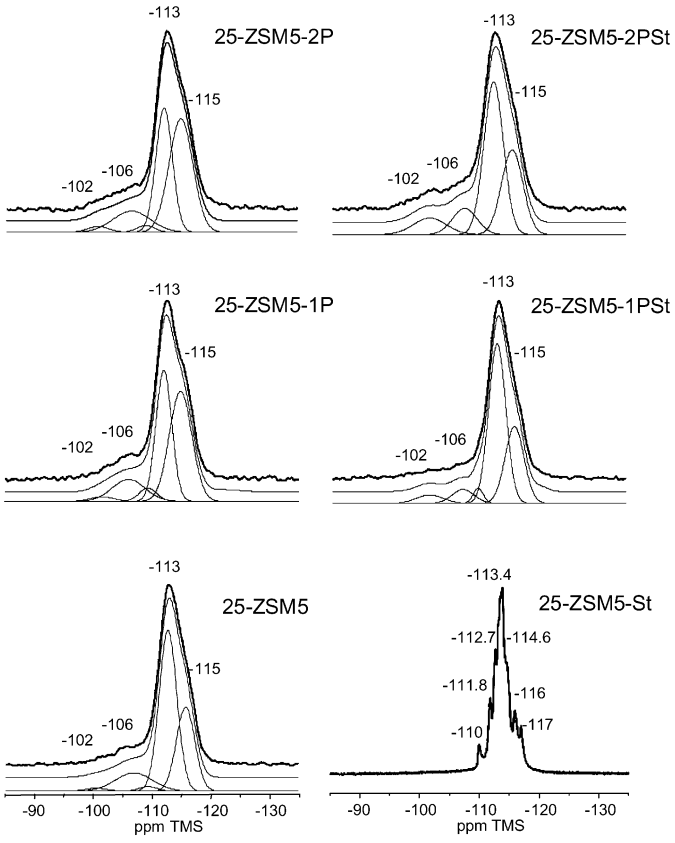

Fig. 2. ^{29}Si MAS NMR spectra of P-free and P-containing zeolite 25-ZSM5 prepared by impregnation with $NH_4H_2PO_4$, calcined (left), and then steamed at 750 °C 5 h (right).

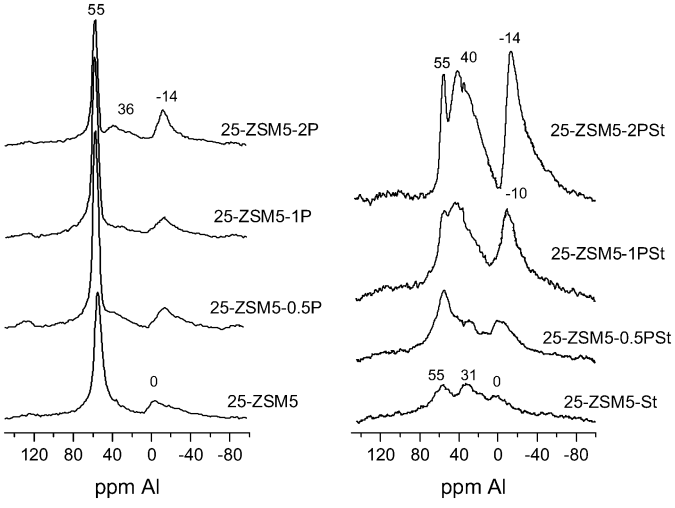

Fig. 3. ^{27}Al MAS NMR spectra of P-free and P-containing zeolite 25-ZSM5 prepared by impregnation with $NH_4H_2PO_4$, calcined (left), and then steamed at 750 °C 5 h (right).

to the formation of $(SiO)_xAl(OP)_{4-x}$ sites by the substitution of some P by Si atoms at high temperature [32,43], and that at −16 ppm has been attributed to octahedral aluminum coordinated to phosphate groups arising from the reaction of phosphoric acid with extra-framework polymeric alumina [44]. We must note that the overall intensity of the spectra of the steamed

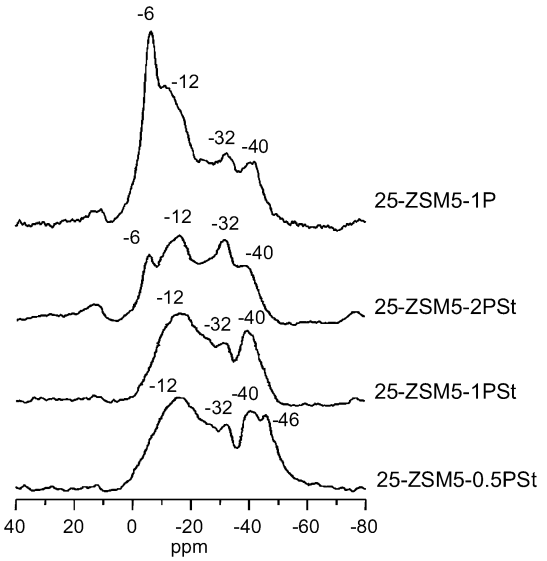

Fig. 4. ^{31}P MAS NMR spectra of and P-containing zeolite 25-ZSM5 prepared by impregnation with $NH_4H_2PO_4$ calcined (sample 25-ZSM5-1P) and steamed at 750 °C 5 h.

zeolites, especially the P-free at low P content, indicates the existence of "invisible" aluminum species in highly distorted environments.

The ^{31}P MAS NMR spectrum of sample 25-ZSM5-1P after calcination (Fig. 4) consists of an intense peak at −6 ppm and three broad signals at −12, −32, and −40 ppm. The peak at −6 ppm is attributed to P in pyrophosphoric acid, pyrophosphates, or terminal groups in short-chain polyphosphates, whereas the −12 ppm signal is related to intermediate groups in short-chain polyphosphates or pyrophosphates [28,30,31,45,46]. The signal at ca. −32 ppm is assigned to amorphous aluminum phosphate [35], and the signal at ∼ −40 ppm is assigned to highly condensed polyphosphate or polyphosphoric species [28,31,45]. P signals in the 30–40 ppm region have also been attributed to $(SiO)_xAl(OP)_{4-x}$ species generated by the substitution of framework Si atoms by P [32]. Moreover, the formation of a silicon pyrophosphate phase involving octahedral silicon appear improbable (^{29}Si NMR signals < −200 ppm not observed) [42,47–49].

The ^{31}P MAS NMR spectra of P-modified ZSM-5 after steaming at 750 °C for 5 h are shown in Fig. 4. As shown for 25-ZSM5-1PSt, the relative intensity of low field signals decreases whereas that of the high field signals increases after steaming, indicating the transformation of less-condensed polyphosphates or polyphosphoric acid in others more condensed. Another signal appearing at −46 ppm in the steamed sample containing 0.5% P has been assigned to intermediate P_4O_{10} groups [31,47]. The signal corresponding to aluminum phosphate at ca. −30 ppm, seems to increase slightly with P content.

Although the interpretation of the NMR spectra of P-containing zeolites is still being debated, the results presented here allow us to state the following conclusions:

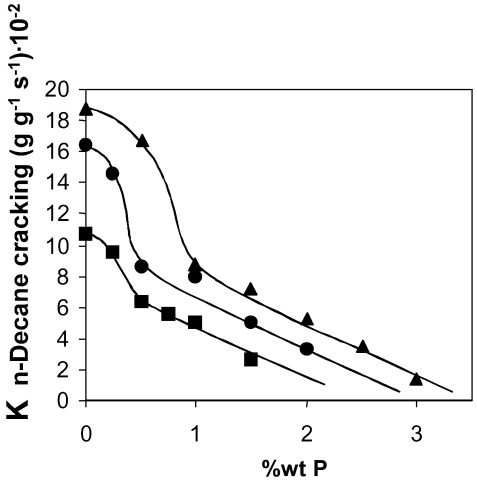

Fig. 5. First order kinetic rate constants in the cracking of *n*-decane of P-free and P-containing zeolite 25-ZSM5 prepared by impregnation with $NH_4H_2PO_4$, after calcination (▲) 15-ZSM5-P, (●) 25-ZSM5-P, (■) 40-ZSM5-P.

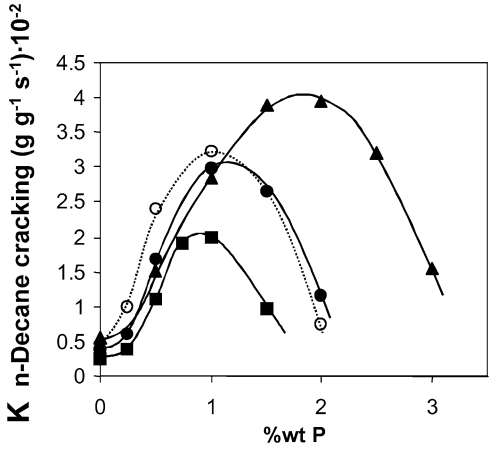

Fig. 6. First order kinetic rate constants in the cracking of *n*-decane of P-free and P-containing zeolite 25-ZSM5 prepared by impregnation with $NH_4H_2PO_4$, and steamed at 750 °C 5 h: (▲) 15-ZSM5-P, (●) 25-ZSM5-P, (■) 40-ZSM5-P, and in form of H_3PO_4: (○) 25-ZSM5-A.

1. A clear increase in the Si/Al framework ratio after P impregnation and calcination is not evident from the NMR spectra.
2. The presence of P prevents zeolite dealumination during steaming to the same extent as on the unmodified ZSM-5 zeolite.
3. The stability of framework Al increases with P content.
4. An amorphous extra-framework aluminophosphate is formed during the dealumination process under steaming.
5. Various phosphorus-containing species, more condensed after steaming, are evident from the ^{31}P NMR spectra.

3.3. Catalytic activity: *n*-decane cracking

Now, taking into account all of the characterization results given earlier, we should be able to predict the catalytic behaviour of the P-modified ZSM-5 zeolites. Because the acidity of the calcined samples, especially the stronger acidity that retains pyridine at 350 °C, decreases with P content, the same trend is expected for the activity in *n*-decane cracking. However, the opposite is expected for steamed samples: lower activity for unmodified ZSM-5 and increased activity with P content.

Fig. 5 shows the *n*-decane cracking constant rate as a function of the wt% of P for calcined P-free and P-containing ZSM-5 catalysts. As predicted from the acidity measurements given in Tables 3–5, the activity of the P-containing zeolites decreases as the P content increases. The differences observed among the zeolites with different Si/Al ratios suggest that a higher amount of P is required to reach similar reductions in activity for samples richer in aluminum.

The rate constants of the reaction on the steamed P-free and P-containing ZSM-5 are plotted as functions of the P content in Fig. 6. The activity of the P-free zeolites is much lower after steaming than in its calcined state (see Fig. 5), in agreement with the sharp acidity loss resulting from the strong zeolite dealumination. The zeolite activity of steamed P-modified ZSM-5 first increases and then decreases as the P content increases, reaching a maximum at around 0.75, 1, and 2 wt% for 40-ZSM5, 25-ZSM5, and 15-ZSM5, respectively. This optimum P content corresponds to a P/Al molar ratio of 0.5–0.7 for the three series of ZSM-5. For samples 25-ZSM5-P, similar results are obtained irrespective of the P source ($NH_4H_2PO_4$ or H_3PO_4).

The decrease in the catalytic activity at high P loading could be due to diffusional problems of reactant and products within the pores because of the presence of non-framework species. Indeed, a reduced effective pore diameter in sample ZSM5/P has been reported to enhance *p*-xylene selectivity in toluene alkylation and xylene isomerization reactions [21,22]. But the micropore volume of ZSM-5 at high P loading, shown in Tables 3–5, is not sensibly reduced at high phosphorus loading, suggesting that this is not the main reason for the observed activity reduction. An alternative explanation could be the decrease in catalyst acidity (Tables 3–5). However, although it is true that the medium and weak acidity of steamed P-containing zeolites increase with P content, the evolution of the strong acid sites is not clear, because of its low intensity.

As mentioned earlier, the acidity of the steamed P-containing samples is partially restored by washing with NH_4Cl or NH_4F, as shown for 25-ZSM5-1PSt in Table 6. The catalytic results for 25-ZSM5-1PSt before and after washing are compared in Fig. 7. A sharp increase in catalytic activity is observed when the sample acidity is partially recovered by washing. A similar experiment done with the P-free 25-ZSM5-St sample revealed that neither acidity (see Table 6) nor cracking activity increased after washing, even though an appreciable amount of aluminum was leached. From these experiments, it seems reasonable to consider that phosphorus compounds interact with the acid sites in ZSM-5, neutralizing the acidity in a reversible manner that probably is not so different than the effect achieved by cationic exchange.

From the results presented above, it appears that *n*-decane cracking is a very sensitive reaction test for the presence of strong acid sites in low concentrations, which are difficult to observe by other methods, such as the adsorption/desorption of pyridine using IR spectroscopy.

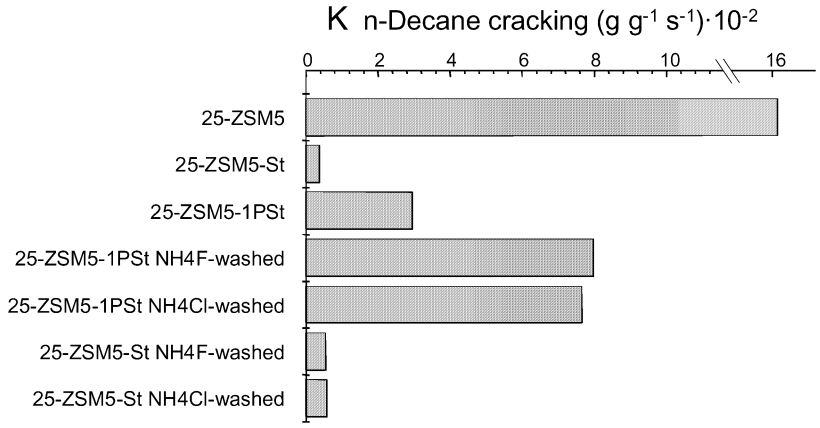

Fig. 7. First order kinetic rate constants in the cracking of *n*-decane on zeolites 25-ZSM5, 25-ZSM5-St, 25-ZSM5-1PSt and the steamed samples ammonium exchanged with NH_4Cl or NH_4F.

Table 7
Yields and ratios of interest interpolated at 40% of total conversion and first order kinetic rate constant in the cracking of *n*-decane at 500 °C, 60 s TOS, on ZSM-5 steamed and P-ZSM5-steamed samples impregnated with the optimum amount of phosphorus. Influence of Si/Al ratio of parent ZSM-5 and phosphorus source

	15-ZSM5-St	25-ZSM5-St	40-ZSM5-St	15-ZSM5-2PSt	25-ZSM5-1PSt	25-ZSM5-1ASt	40-ZSM5-1PSt
K (s^{-1})	0.55	0.38	0.25	3.96	2.97	3.21	1.99
Total C_{5+} (wt%)	7.2	7.6	5.9	11.6	11	9.2	10.5
Gases C_1–C_4 (wt%)	28.5	26.5	26.5	27.7	27.5	29.7	27.9
Coke (wt%)	4.3	5.6	7.6	0.7	1.5	1	1.7
Gases composition (wt%)							
$C_1 + C_2$	2.96	2.95	3.51	1.60	2.13	2.08	2.01
Propane	4.56	3.99	2.94	5.79	5.56	6.33	5.15
Propylene	9.18	8.80	9.75	6.74	7.15	7.60	7.95
Isobutane	1.09	0.74	0.40	2.21	1.86	2.19	1.64
n-Butane	2.95	2.57	2.12	4.01	3.63	4.04	3.52
Total butenes	7.72	7.38	7.69	7.29	7.11	7.47	7.56
Isobutene	3.23	3.19	3.17	3.24	3.10	3.33	3.22
Ratios							
Propylene/propane	2.01	2.21	3.31	1.16	1.29	1.20	1.54
Butenes/butanes	1.91	2.23	3.05	1.17	1.30	1.20	1.47
Isobutene/isobutane	2.95	4.31	9.20	1.47	1.67	1.52	1.97
$C_1 + C_2$/isobutane	2.71	3.99	8.71	0.73	1.15	0.95	1.23
C_3/C_4	1.17	1.20	1.24	0.93	1.01	1.02	1.03

The modification of ZSM-5 with P has an effect not only on the cracking activity, but also on the selectivity of the steamed samples. Table 7 gives the distribution of *n*-decane cracking products at constant conversion on steamed P-ZSM5 samples, with different Si/Al ratios and prepared with $NH_4H_2PO_4$ or H_3PO_4. It is evident that the formation of dry gas and coke is reduced on the P-containing samples. For the steamed P-free ZSM-5 zeolites, the propylene/propane, butenes/butanes, and isobutene/isobutane ratios increase as the framework Al of the starting zeolite decreases, diminishing sharply on the P-containing samples. The lower olefinicity of P-ZSM-5 is fully compensated for by this sample's much higher activity and lower selectivity to dry gas. These results are consistent with the preservation of a larger number of acid sites on P-containing samples.

Continuing to analyse the selectivity pattern summarized in Table 7, we see that the $C_1 + C_2$/isobutane ratio, accounting for the protolytic versus beta-scission cracking mechanism, increases as the Si/Al ratio of the parent zeolite increases. The dramatic diminution for the P-containing samples agrees with their higher acidity. The C_3/C_4 ratio, representing a cracking-to-disproportionation ratio, depends on the channel's size or tortuosity. This ratio is lower in the P-free catalysts, indicating that adding P does not narrow the size of the channel, at least to a point of restricting the formation of isobutyl cations.

3.4. Hypothesis for the phosphorus stabilization effect

From catalyst characterization and activity results, we can try to rationalize the interaction of phosphorus with the zeolite surface and its effect on the *n*-decane cracking reactivity. Characterization of the P-containing ZSM-5 zeolites reveals the coexistence of different species resulting from interaction with the zeolite. Although there is general agreement as to the formation of an extra-framework aluminophosphate phase during framework dealumination, different models have been proposed to explain the experimental results. Fig. 8A depicts the species resulting from the interaction of phosphorus with a

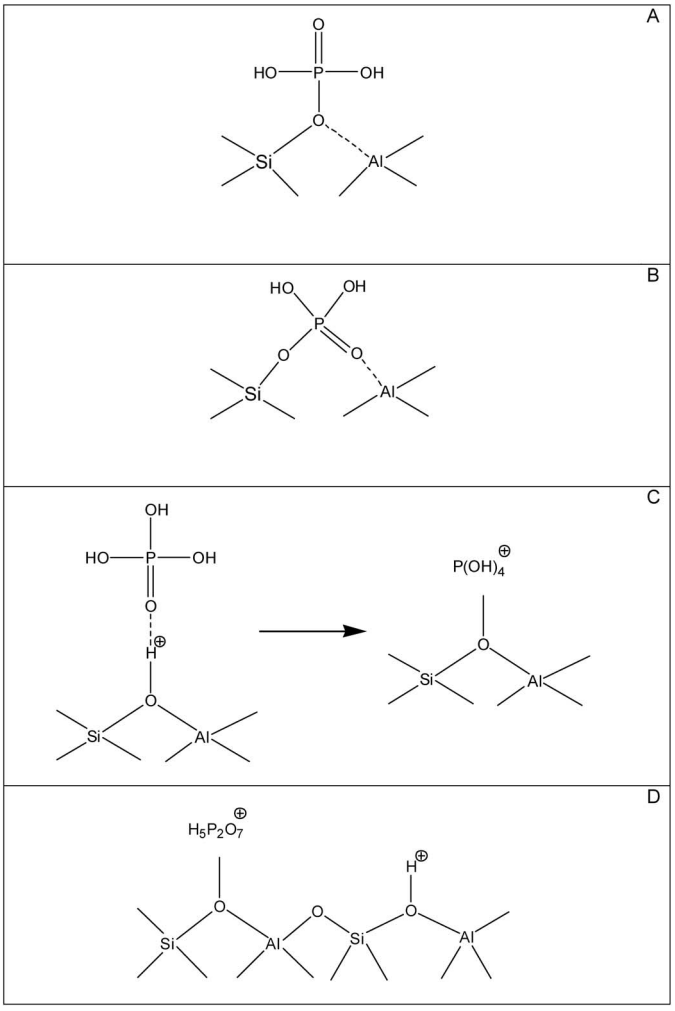

Fig. 8. Models proposed for the interaction of phosphorus with the Brönsted acid sites of ZSM-5 prepared by impregnation with orthophosphoric acid or ammonium phosphates and calcination, as proposed by (A) Védrine et al. [26], Kaeding et al. [23], (B) Lercher et al. [27], (C), (D) this article.

zeolite Brönsted acid site, as suggested earlier by Védrine et al. [26] and Kaeding et al. [23]. Fig. 8B shows an alternative model involving a direct bond between a P atom and the oxygen of the Si–O–Al group by breaking the Al–O bond [27] and then opening the zeolite framework. Zhuang et al. [32] suggested substituting framework silicon by phosphorus atoms into the zeolite positions, leading to units of the type $(SiO)_xAl(OP)_{4-x}$ ($x = 1$–4), which would proceed up to the segregation of an aluminophosphate phase. Note that for $x = 3$, the resulting center is similar to those shown in Figs. 8A and B [27]. But the species depicted in Figs. 8A and B require breakage of the Si–O–Al bond and appear to be difficult to revert by single cationic exchange or hot-water washing. An alternative model involving ionic interaction between phosphorus and the zeolite is needed to explain our experimental results. Accordingly, phosphorus could be incorporated into ZSM-5 through the formation of a tetrahydroxyphosphonium cation $P(OH)_4^+$ via protonation of the orthophosphoric acid by the zeolite Brönsted sites (Fig. 8C). This ion has been proven to exist in HNO_3 or H_2SO_4 solutions [53–55], and it can be assumed that the acidity of ZSM-5 is strong enough to protonate the orthophosphoric acid. Once the ion is formed, it could lose one molecule of water, giving the dihydroxyoxophosphonium cation $PO(OH)_2^+$, or could form dimmers or oligomers with one or more molecules of orthophosphoric acid (as in, e.g., the protonated pyrophosphoric acid $H_5P_2O_7^+$) (Fig. 8D).

According to our model (Figs. 8C and D), in calcined P-containing ZSM-5, phosphorus is mainly forming cationic pyrophosphate or short-chain polyphosphate (see ^{31}P NMR), partially neutralizing the Brönsted zeolite acidity. Through exchange or neutralization of the acid sites, the corresponding aluminum is stabilized in the framework, as occurs when protons are exchanged by rare earth or other cations [56–58]. After steaming, framework dealuminization proceeds (albeit to a lesser extent than in the P-free zeolites), producing aluminum phosphate and forming more condensed pyrophospates. The pyrophosphate or polyphosphate species (at least some of them) will be cationic and removable by washing, leading to at least partial recovery of zeolite acidity [31]. If all of the acid sites were neutralized with P species, then zeolite acidity would be lost, making the acidity of the P–OH groups too weak to retain pyridine at 350 °C or to crack *n*-decane. The resulting zeolite would not have sufficient acidity to perform reactions demanding high acid strength while still containing aluminum at framework sites. This is exactly what occurs in steamed samples containing an excess of phosphorus. Although framework aluminum is present, the acidity and especially the cracking activity are very low. The acidity and catalytic activity are restored after washing, however.

Now consider the stabilizing effect of phosphorus. Following the above reasoning, the acidity of the P-containing zeolites must come from the framework aluminum atoms not "neutralized" by phosphorus. This means that not only the aluminum atoms directly interacting with phosphorus, but also other atoms, likely in close proximity, must be stabilized. In an hypothetical ideal situation, we can imagine an "Al-pair" [Al–O–Si–O–Al or Al–O–(Si–O)$_2$–Al] with one of the associated Brönsted sites neutralized by phosphorus species, which has an stabilizing effect on the second aluminum. If this were the case, then we could expect an optimum in acidity for an overall P/Al ratio of 0.5. According to this hypothesis, the stabilizing effect of phosphorus would be greater in zeolites containing a large number of Al pairs, as is frequently found in zeolite ZSM-5, especially at high Al content [50–52]. Experimentally, we observe maximum cracking activity at a P/Al ratio of around 0.5, higher for samples with a lower Si/Al ratio (see Fig. 6), which are expected to have more Al pairs. Therefore, although we have described an ideal situation, the general trends of our results agree with those of the model and point out that the stabilization effect is enhanced in samples containing "Al pairs."

3.5. Stabilization of zeolite ZSM-5 as fluid catalytic cracking additive

The preservation of framework aluminum and acidity on calcined P-impregnated ZSM-5 zeolite must necessarily have a significant affect on their performance as FCC additives. We

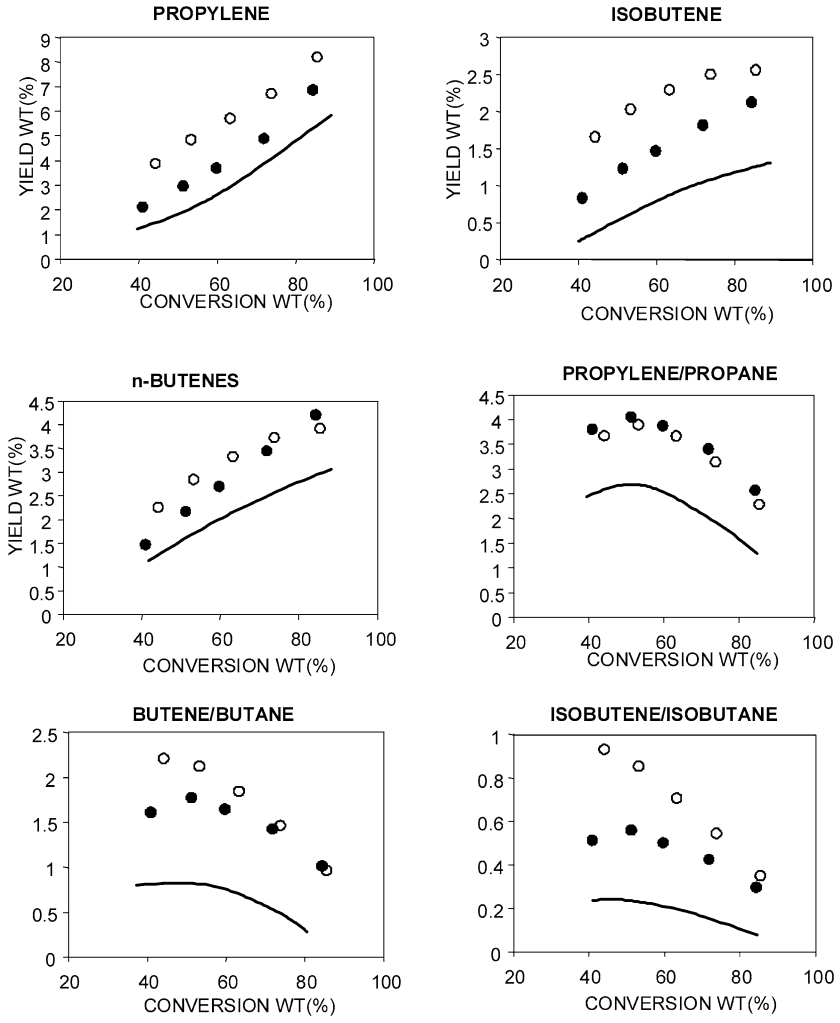

Fig. 9. C_3–C_4 selectivities and ratios of interest in the cracking of gasoil at 520 °C and 30 s time on stream over (line) USY-2.426 nm as base catalyst and (●) 25-ZSM5-St and (○) 25-ZSM5-1PSt at 750 °C for 5 h at 13.3 wt% of additive level.

tested the sample 25-ZSM5-1PSt (in the form of $NH_4H_2PO_4$) steamed as an additive of a USY zeolite (unit cell size, 2.426 nm) for the cracking of a commercial vacuum gasoil (see the composition in Table 2). Comparing the results with those for steamed ZSM-5 without phosphorus indicates that phosphorus has a much greater effect on product selectivity than on *n*-decane cracking (Fig. 9). In the case of vacuum gasoil, the yields of propylene, total butene, and isobutene are higher when the steamed ZSM-5 additive contains phosphorus. The olefinicity ratios (especially the isobutene/isobutane ratio) are higher when the P-stabilized ZSM-5 is used. It is clear that the activity of ZSM-5 as an FCC additive is significantly increased when stabilized by the addition of the optimum amount of phosphorus.

4. Conclusions

We have shown that phosphorus impregnation in the form of either $NH_4H_2PO_4$ or H_3PO_4 stabilizes the framework aluminum of zeolite ZSM-5 against severe hydrothermal treatment. More Brönsted acidity is preserved, and the P-containing zeolites show higher activity for the cracking of *n*-decane. The proportion of acid sites preserved after steaming by P impregnation depends on the amount of phosphorus added and reaches an optimum for a P/Al molar ratio of around 0.5–0.7. When phosphorus is added in excess of the optimum amount, more framework aluminum is stabilized, but the acidity and activity decrease significantly.

This behavior can be explained with a model involving a phosphorus–zeolite interaction in which cationic species of phosphorus, formed by protonation of orthophosphoric acid, neutralize one of the acid sites corresponding to a framework Al pair, stabilizing this aluminum while its neighbor preserves its acidity toward steaming. ZSM-5 stabilized with phosphorus used after steaming as an FCC catalyst additive has shown markedly higher activity than the P-free ZSM-5 with higher yields of propylene and butenes.

Acknowledgment

The authors thank CICYT (MAT 2003-07945-C02-01) for financial support.

References

[1] S.I. Zones, S.J. Hwang, S. Elomari, I. Ogino, M.E. Davis, A.W. Burton, C. R. Chimie 8 (2005) 267.
[2] A. Burton, S. Elomari, C.Y. Chen, R.C. Medrud, I.Y. Chan, L.M. Bull, C. Kibby, T.V. Harris, S.I. Zones, E.S. Vittoratos, Chem. Eur. J. 9 (2003) 5737.
[3] K.G. Strohmaier, D.E.W. Vaughan, J. Am. Chem. Soc. 125 (2003) 16035.
[4] A. Corma, M. Diaz-Cabañas, J. Martinez-Triguero, F. Rey, J. Rius, Nature 418 (2002) 514.
[5] A. Corma, F. Rey, J. Rius, M.J. Sabater, S. Valencia, Nature 431 (2004) 287.
[6] J.L. Paillaud, B. Harbuzaru, J. Patarin, N. Bats, Science 304 (2004) 990.
[7] A. Corma, M.J. Diaz-Cabañas, F. Rey, S. Nicolooulas, K. Boulahya, Chem. Commun. (2004) 1356.
[8] A. Corma, M.E. Davis, Chem. Phys. Chem. 5 (2004) 304.
[9] J. Scherzer, J.L. Bass, J. Catal. 46 (1977) 100.
[10] N.Y. Chen, T.O. Mitchell, D.H. Olson, B.P. Pelrine, IEC Prod. Res. Dev. 16 (1977) 247.
[11] J. Scherzer, R.E. Ritter, IEC Prod. Res. Dev. 17 (1978) 219.
[12] F. Lemos, F.R. Ribeiro, M. Kern, G. Giannetto, M. Guisnet, Appl. Catal. 39 (1988) 227.
[13] T.G. Roberie, J.F. Terbot, US Patent 5 194 412 (1991).
[14] R.P.L. Absil, J.A. Herbst, US Patent 5 231 064 (1991).
[15] E.J. Demmel, US Patent 5 288 739 (1993).
[16] A. Corma, V. Fornes, W. Kolodziejski, L.J. Martinez-Triguero, J. Catal. 145 (1994) 27.
[17] N.Y. Chen, W.W. Kaeding, F.G. Dwyer, J. Am. Chem. Soc. 101 (1979) 6783.
[18] M. Derewinski, J. Haber, J. Ptaszynski, V.P. Shiralkar, S. Dzwigaj, Stud. Surf. Sci. Catal. 18 (1984) 209.
[19] A. Jentys, G. Rumplmayr, J.A. Lercher, Appl. Catal. 53 (1989) 299.
[20] A. Jentys, G. Rumplmayr, H. Vinek, J.A. Lercher, Heterog. Catal. 6 (2) (1987) 264.
[21] W.W. Kaeding, C. Chu, L.B. Young, B. Weinstein, S.A. Butter, J. Catal. 67 (1981) 159.
[22] W.W. Kaeding, C. Chu, L.B. Young, S.A. Butter, J. Catal. 69 (1981) 392.
[23] W.W. Kaeding, S.A. Butter, J. Catal. 61 (1980) 155.
[24] J.A. Lercher, G. Rumplmayr, Appl. Catal. 25 (1986) 215.
[25] J.A. Lercher, G. Rumplmayr, H. Noller, Acta Phys. Chem. 31 (1985) 71.
[26] J.C. Vedrine, A. Auroux, P. Dejaifve, V. Ducarme, H. Hoser, S. Zhou, J. Catal. 73 (1982) 147.
[27] H. Vinek, G. Rumplmayr, J.A. Lercher, J. Catal. 115 (1989) 291.
[28] J. Caro, M. Bülow, M. Derewinski, J. Haber, M. Hunger, J. Kärger, H. Pfeifer, W. Storek, B. Zibrowius, J. Catal. 124 (1990) 367.
[29] G. Seo, R. Ryoo, J. Catal. 124 (1990) 224.
[30] G. Oehlmann, H.G. Jerschkewitz, G. Lischke, R. Eckelt, B. Parlitz, E. Schreier, B. Zibrowius, E. Loeffler, Stud. Surf. Sci. Catal. 65 (1991) 1.
[31] G. Lischke, R. Eckelt, H.G. Jerschkewitz, B. Parlitz, E. Schreier, W. Storek, B. Zibrowius, G. Oehlmann, J. Catal. 132 (1991) 229.
[32] J. Zhuang, D. Ma, G. Yang, Z. Yan, X. Liu, X. Liu, X. Han, X. Bao, P. Xie, Z. Liu, J. Catal. 228 (2004) 234.
[33] C.A. Emeis, J. Catal. 141 (1993) 347.
[34] A. Corma, J. Martinez-Triguero, S. Valencia, E. Benazzi, S. Lacombe, J. Catal. 206 (2002) 125.
[35] F.M. Bautista, J.M. Campelo, A. Garcia, D. Luna, J.M. Marinas, A.A. Romero, Appl. Catal. A 96 (1993) 175.
[36] B. Rebenstorf, T. Lindblad, S.L. Andersson, J. Catal. 128 (1991) 293.
[37] Z. Yan, D. Ma, J. Zhuang, X. Liu, X. Liu, X. Han, X. Bao, F. Chang, L. Xu, Z. Liu, J. Mol. Catal. A 194 (2003) 153.
[38] J.X. Chen, T.H. Chen, N.J. Guan, J.Z. Wang, Catal. Today 93–95 (2004) 627.
[39] S.M.C. Menezes, V.L. Camorim, Y.L. Lam, R.A.S. San Gil, A. Bailly, J.P. Amoureux, Appl. Catal. A 207 (2001) 367.
[40] T.H. Chen, B.H. Wouters, P.J. Grobet, Eur. J. Inorg. Chem. 2 (2000) 281.
[41] J. Caro, M. Bulow, M. Derewinski, M. Hunger, J. Karger, U. Kurschner, H. Pfeifer, W. Storek, B. Zibrowius, Stud. Surf. Sci. Catal. 52 (1989) 295.
[42] Y. Shu, D. Ma, X. Bao, Y. Xu, Catal. Lett. 66 (2000) 161.
[43] Y. Shu, D. Ma, X. Liu, X. Han, Y. Xu, X. Bao, J. Phys. Chem. B 104 (2000) 8245.
[44] L.D. Quin, M. Borbaruah, G.S. Quin, L.C. Dickinson, S. Jankowski, Heteroatom. Chem. 9 (1998) 691.
[45] T.M. Duncan, D.C. Douglass, Chem. Phys. 87 (1984) 339.
[46] A.R. Grimmer, U. Haubenreisser, Chem. Phys. Lett. 99 (1983) 487.
[47] G.D. Cody, B. Mysen, G. Saghi-Szabo, J.A. Tossell, Geochim. Cosmochim. Acta 65 (2001) 2395.
[48] B.A. Morrow, S.J. Lang, I.D. Gay, Langmuir 10 (1994) 756.
[49] T.R. Krawietz, P. Lin, K.E. Lotterhos, P.D. Torres, D.H. Barich, A. Clearfield, J.F. Haw, J. Am. Chem. Soc. 120 (1998) 8502.
[50] J. Dedecek, D. Kaucky, B. Wichterlova, Chem. Commun. (2001) 970.
[51] J. Dedecek, D. Kaucky, B. Wichterlova, O. Gonsiorova, Phys. Chem. Chem. Phys. 4 (2002) 5406.
[52] J. Dedecek, V. Gabova, B. Wichterlova, Stud. Surf. Sci. Catal. 142B (2002) 1817.
[53] C.C. Addison, J.W. Bailey, S.H. Bruce, M.F.A. Dove, R.C. Hibbert, N. Logan, Polyhedron 2 (1983) 651.
[54] R.C. Hibbert, N. Logan, J. Chem. Soc. Dalton Trans. (1985) 865.
[55] R.J. Gillespi, R. Kapoor, E.A. Robinson, Can. J. Chem. 44 (1966) 1203.
[56] J.N. Armor, T.S. Farris, Appl. Catal. B 4 (1994) L11–L17.
[57] A.A. Lappas, C.S. Triantafillidis, Z.A. Tsagrasouli, V.A. Tsiatouras, I.A. Vasalos, N.P. Evmiridis, Stud. Surf. Sci. Catal. 142A (2002) 807.
[58] Y. Yoshimura, N. Kijima, T. Hayakawa, K. Murata, K. Suzuki, F. Mizukami, K. Matano, T. Konishi, T. Oikawa, M. Saito, T. Shiojima, K. Shiozawa, K. Wakui, G. Sawada, K. Sato, S. Matsuo, N. Yamaoka, Catal. Surv. Jpn. 4 (2001) 157.